Measuring and Suppressing Quantum State Leakage in a Superconducting Qubit

Zijun Chen,[1] Julian Kelly,[2] Chris Quintana,[1] R. Barends,[2] B. Campbell,[1] Yu Chen,[2] B. Chiaro,[1] A. Dunsworth,[1] A. G. Fowler,[2] E. Lucero,[2] E. Jeffrey,[2] A. Megrant,[1,3] J. Mutus,[2] M. Neeley,[2] C. Neill,[1] P. J. J. O'Malley,[1] P. Roushan,[2] D. Sank,[2] A. Vainsencher,[1] J. Wenner,[1] T. C. White,[1] A. N. Korotkov,[4] and John M. Martinis[1,2,*]

[1]*Department of Physics, University of California, Santa Barbara, California 93106-9530, USA*

[2]*Google Inc., Santa Barbara, California 93117, USA*

[3]*Department of Materials, University of California, Santa Barbara, California 93106, USA*

[4]*Department of Electrical and Computer Engineering, University of California, Riverside, California 92521, USA*

(Received 22 September 2015; published 13 January 2016)

Leakage errors occur when a quantum system leaves the two-level qubit subspace. Reducing these errors is critically important for quantum error correction to be viable. To quantify leakage errors, we use randomized benchmarking in conjunction with measurement of the leakage population. We characterize single qubit gates in a superconducting qubit, and by refining our use of derivative reduction by adiabatic gate pulse shaping along with detuning of the pulses, we obtain gate errors consistently below 10^{-3} and leakage rates at the 10^{-5} level. With the control optimized, we find that a significant portion of the remaining leakage is due to incoherent heating of the qubit.

DOI: 10.1103/PhysRevLett.116.020501

Accurate manipulation of the states in a quantum two-level system (qubit) is a key requirement for building a fault tolerant quantum processor [1]. However, many physical quantum systems, such as quantum dots [2] and superconducting qubits [3], have multiple levels from which two levels are chosen to form the computational subspace. The presence of noncomputational levels leads to two types of errors: leakage errors, where the quantum state populates noncomputational levels, and phase errors due to coupling of computational and noncomputational levels when driven by control fields [4,5]. Previous experimental work [6,7] on superconducting qubits has focused on reducing phase errors, because they were the dominant source of total gate infidelity. Indeed, the suppression of phase errors using derivative reduction by adiabatic gate (DRAG) pulse shaping [8] has helped push single qubit fidelity in superconducting qubits over 99.9% [9,10].

However, gate fidelity is not the only metric that determines the viability of quantum error correction (QEC) because certain errors are more deleterious than others. Specifically, leakage errors are highly detrimental to error correcting codes such as the surface code, because interactions with a qubit in a leakage state have a randomizing effect on the interacting qubits [11]. Moreover, leakage states can be as long-lived as the qubit states, leading to time-correlated errors which further degrade performance [12]. These concepts were recently demonstrated in a 9 qubit repetition code [13], where single leakage events persisted for multiple error detection cycles and propagated errors to neighboring qubits. Understanding and reducing leakage is of critical importance for realizing QEC.

In this Letter, we characterize single qubit leakage errors in a superconducting qubit. To estimate leakage errors, we use randomized benchmarking (RB) [14–17] in conjunction with measurements of leakage state populations. Using this method, we show that previous experimental realizations of DRAG pulse shaping have a trade-off between total fidelity and leakage errors. We overcome this trade-off using additional pulse shaping, and obtain gates that have both state-of-the-art fidelity and low leakage. Additionally, we use RB to measure the dependence of leakage on pulse length.

Our experiment uses Clifford-based randomized benchmarking [15], which is typically used to characterize average gate fidelity. In Clifford-based RB, we apply a random sequence of gates chosen from the single qubit Clifford group, which is the group of rotations that map the six axial Bloch states to each other. We then append a recovery Clifford gate to the end of the sequence such that the complete sequence is ideally the identity operation. Thus, the fidelity of a sequence is the probability of mapping $|0\rangle$ to $|0\rangle$. By randomly choosing the gates in each sequence, phase and amplitude errors accumulate incoherently, which leads to exponential decay of the sequence fidelity with increasing sequence length. The crux of our protocol is that randomization also accumulates leakage errors incoherently [18], such that over many gates we build up leakage populations to a level that can be measured using current techniques. We note that leakage as discussed here differs from irreversible loss of the qubit; RB in the presence of loss was previously discussed in Ref. [22].

For our test bed we use a single Xmon transmon qubit [23,24] (Q_7) from the 9 qubit chain described in Ref. [13]. The transmon has a weakly anharmonic potential, shown in Fig. 1(a), which supports a ladder of energy levels. The two lowest levels form our qubit, and the primary

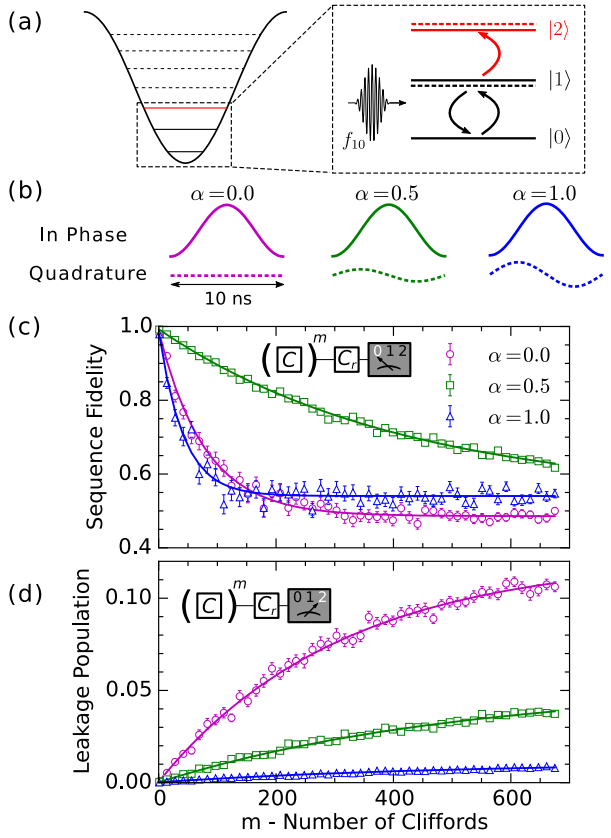

FIG. 1. (a) Weakly anharmonic potential of a transmon. When driving $|0\rangle$ to $|1\rangle$, direct excitation to $|2\rangle$ (red arrow) causes leakage errors, while ac Stark repulsion of the $1\leftrightarrow2$ transition (dashed lines) leads to phase errors. (b) Simple DRAG correction, which adds the derivative of the envelope to the quadrature component of the envelope. Three different DRAG weightings (α) are shown. (c) Exponential decay of sequence fidelity from randomized benchmarking, shown for the three values of α. Each point is the average of 75 different random sequences. Fidelity is highest for $\alpha = 0.5$ (d) $|2\rangle$ state population versus sequence length, showing accumulation of leakage with sequence length. Leakage is lowest for $\alpha = 1.0$.

noncomputational level is the $|2\rangle$ state. Leakage errors arise when the qubit state is directly excited to the $|2\rangle$ state, while phase errors occur due to ac Stark shifting of the $1\leftrightarrow2$ transition [4]. We use the transmon because of its demonstrated coherence and tunability [23,25]. Alternatively, leakage can be suppressed by engineering qubits with larger anharmonicities such as flux qubits, which have recently also achieved high coherence [26].

We operate the qubit at a frequency f_{10} of 5.3 GHz, and the anharmonicity $\Delta = \omega_{21} - \omega_{10}$ is $2\pi \times -212$ MHz. Microwave (XY) control is achieved using a capacitively coupled transmission line driven at the qubit frequency. We generate control pulses using a custom arbitrary waveform generator, and the pulses are shaped with a cosine envelope. We measure the qubit state using a dispersive readout scheme [27] in conjunction with a bandpass filter [28] and a wideband parametric amplifier [29]. This setup allows us to discriminate the $|2\rangle$ state in addition to the two computational levels with high fidelity [18]. The T_1 of the device at the operating frequency is 22 μs, while a Ramsey experiment shows two characteristic decay times [30], an exponential decay time T_{ϕ_1} of 8 μs and a Gaussian decay time T_{ϕ_2} of 1.8 μs.

To illustrate our novel use of RB, we begin by measuring how DRAG suppresses leakage and phase errors. We use the simplified version of DRAG described in Refs. [6,7]. Given a control envelope $\Omega(t)$, we add the time derivative $\dot{\Omega}(t)$ to the quadrature component:

$$\Omega'(t) = \Omega(t) - i\alpha\frac{\dot{\Omega}(t)}{\Delta}, \tag{1}$$

where α is a weighting parameter. Fourier analysis [4,31] shows that the DRAG correction suppresses the spectral weight of the control pulse at the $1\leftrightarrow2$ transition if $\alpha = 1.0$, which minimizes leakage errors. However, the optimal value to compensate the ac Stark shift and correct for phase errors is $\alpha = 0.5$ [4,6].

We confirm these concepts by performing Clifford-based RB using 10 ns microwave pulses shaped with three different values of α (0, 0.5, and 1.0), as shown in Fig. 1(b). We combine up to three pulses to form a single Clifford gate; on average, each Clifford gate contains $1.5\,\pi/2$ pulses and $0.375\,\pi$ pulses, resulting in an average gate length of 18.75 ns. Figure 1(c) shows sequence fidelity decay curves for the three values of α. As expected, using $\alpha = 0.5$ yields higher fidelities than $\alpha = 0.0$ or $\alpha = 1.0$. We quantify this improvement using the characteristic scale of the decay p, obtained by fitting to $Ap^m + B$, where A and B encapsulate state preparation, measurement, and recovery errors. We then estimate the error per Clifford as $r_{\text{Clifford}} = (1-p)/2$ [15]. For $\alpha = 0.5$, we obtain an error per Clifford of $(9.6 \pm 0.1) \times 10^{-4}$, while for $\alpha = 0.0$ and $\alpha = 1.0$ we obtain errors of $(6.3 \pm 0.2) \times 10^{-3}$ and $(1.20 \pm 0.01) \times 10^{-2}$ per Clifford, respectively.

Simultaneously, we characterize leakage errors in our gate set from the dynamics of the $|2\rangle$ state measured while performing RB, as shown in Fig. 1(d). For all three values of α, the $|2\rangle$ state population shows an exponential approach to a saturation population. Without correction, this saturation population is significant at about 10%, but decreases by a factor of 3 for $\alpha = 0.5$ and by a factor of 10 for $\alpha = 1.0$. To quantify the leakage rate per Clifford, we fit the $|2\rangle$ state dynamics to a simple rate equation that takes into account leakage from the computational subspace into the $|2\rangle$ state and decay from $|2\rangle$ back into the subspace [18].

$$p_{|2\rangle}(m) = p_\infty(1 - e^{-\Gamma m}) + p_0 e^{-\Gamma m}, \tag{2}$$

$$\Gamma = \gamma_\uparrow + \gamma_\downarrow, \qquad p_\infty = \gamma_\uparrow/\Gamma, \tag{3}$$

where $p_{|2\rangle}(m)$ is the $|2\rangle$ state population as a function of sequence length m, $\gamma_\uparrow$ and $\gamma_\downarrow$ are the leakage and decay rates per Clifford, and p_0 is the initial $|2\rangle$ state population. Using Eq. (2), we extract leakage rates of $(3.92 \pm 0.08) \times 10^{-4}$, $(1.02 \pm 0.02) \times 10^{-4}$, and $(2.18 \pm 0.08) \times 10^{-5}$ for $\alpha = 0$, 0.5 and 1.0.

The results from RB confirm the theory behind simple DRAG: we can minimize either phase error or leakage error, but not both. To simultaneously optimize for both errors, we would like to minimize leakage using simple DRAG, then separately compensate the ac Stark shift. In the original DRAG theory, the Stark shift was compensated using a time-dependent detuning of the qubit [8]. As noted in Refs. [4,5,32], a constant detuning should also be able to compensate the shift [33]. Given an envelope Ω', which may have a quadrature correction, we generate a new envelope,

$$\Omega''(t) = \Omega'(t) e^{2\pi i \delta f t}, \tag{4}$$

where δf is the detuning of the pulse from the qubit frequency. We also redefine the anharmonicity parameter in Eq. (1) to be $\Delta = \omega_{21} - (\omega_{10} + 2\pi\delta f)$, so that leakage suppression still occurs at the $1 \leftrightarrow 2$ frequency. An example of a detuned pulse is shown in Fig. 2(a).

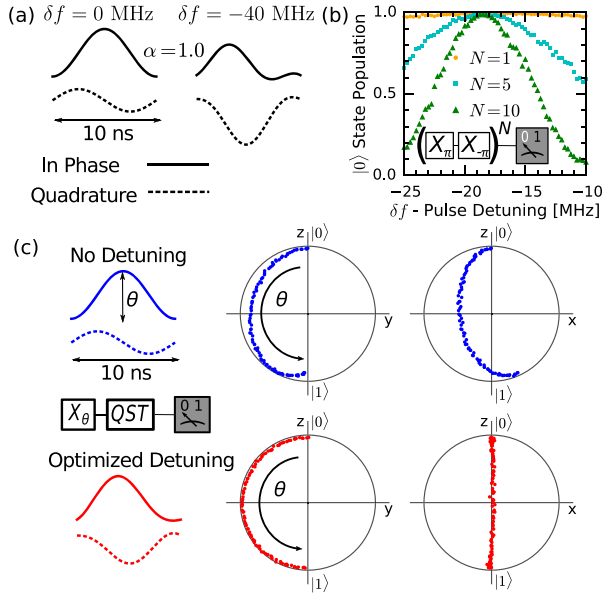

FIG. 2. (a) Control envelopes with simple DRAG with (right) and without (left) detuning of the pulse. The detuning is exaggerated for illustration. (b) We sweep over the detuning δf while performing the pseudoidentity sequence shown in the inset. The sequence maps $|0\rangle$ to $|0\rangle$ when the detuning is optimized. Repeating the sequence increases the sensitivity of the measurement. (c) Quantum state trajectories plotted on projections of the Bloch sphere, with (bottom) and without (top) optimal detuning. The data have been obtained by performing quantum state tomography (QST) after applying a variable X rotation, with the rotation angle ranging from 0 to π.

To optimize the detuning parameter δf, we sweep the detuning of a π pulse while performing the pseudoidentity operation of a π pulse followed by a $-\pi$ pulse along the same rotation axis [6,34]. As shown in Fig. 2(b), the detuning is optimized when the $|0\rangle$ state population is maximized, and the pseudoidentity can be repeated to increase the resolution of the measurement. To verify that the detuning has suppressed phase errors, we perform quantum state tomography after applying a control pulse to our qubit while ramping the amplitude of the pulse, as shown in Fig. 2(c). The Bloch vector only reaches the opposite pole when the detuning is optimized.

We now explore in more detail the dependence of fidelity and leakage on α. In Fig. 3, we show parameters extracted from RB with 10 ns pulses while varying α between 0.0 and 1.5. Without detuning the pulses, we find the minimum error per Clifford to be $(7.9 \pm 3) \times 10^{-4}$ when $\alpha = 0.4$. We note that this is a deviation from the expected optimal value of $\alpha = 0.5$, and the actual optimal value can vary between 0 and 1 for different qubits and operating frequencies. We attribute this deviation to distortions of the pulse between the waveform generator and the qubit [34]. Away from the optimal α, the error increases rapidly.

Next, we optimize the detuning of the pulses for each value of α using the method described in Fig. 2. We find that for π and $\pi/2$ pulses with the same length, the same detuning for both pulses yields the best results. After calibrating the detuning, we recalibrate the pulse amplitudes, then run a short Nelder-Mead optimization on the RB fidelity to get final adjustments to pulse parameters [35]. With these optimizations, we find the average error

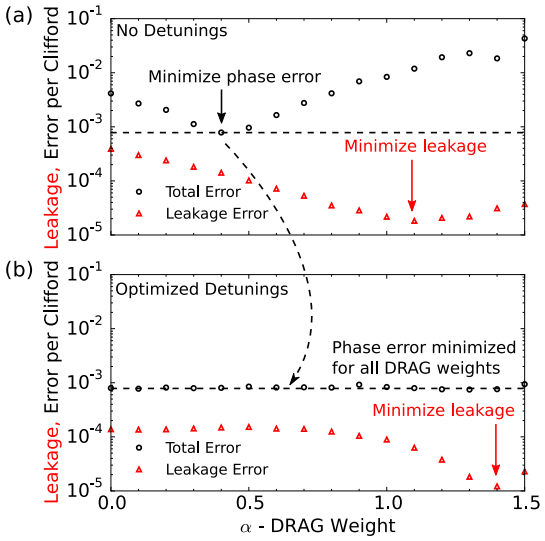

FIG. 3. Total gate fidelity and leakage rates versus DRAG weighting α, measured using RB. (a) Without using pulse detunings, we require different values of α to minimize overall error versus leakage errors. (b) By optimizing our pulses using detunings, we obtain high fidelity for any α, and are free to choose α to minimize leakage.

per Clifford for all values of α to be 9.1×10^{-4}, with a standard deviation of 1×10^{-4}. In other words, we can tune up high fidelity gates for *any* value of α.

With gate fidelity now independent of α, we are free to implement DRAG solely to minimize leakage. Without detuning, the minimum leakage rate is $(1.82 \pm 0.07) \times 10^{-5}$ for $\alpha = 1.1$. After detuning the pulses for optimal fidelity, we see shifts in the leakage rates. For $\alpha > 0.4$, we detune the pulses towards the $1 \leftrightarrow 2$ transition [18], which tends to increase the leakage rate. Nevertheless, we can still suppress leakage to the same level as the undetuned pulses by increasing α to 1.4. Using these parameters, we achieve both high fidelity [$(8.7 \pm 0.4) \times 10^{-4}$ error per Clifford] and low leakage [$(1.2 \pm 0.1) \times 10^{-5}$] [18].

Having characterized 10 ns pulses in detail, we now examine the dependence of leakage on pulse length. As noted previously, pulse detuning can affect the leakage rate; for simplicity, we set the detuning to zero for the following measurements. We initially set $\alpha = 0.0$ and measure the leakage rate while varying the length of our pulses between 8 and 50 ns and calibrating the pulse amplitudes accordingly. We then repeat this measurement with $\alpha = 1.1$ where we previously minimized leakage in Fig. 3(a). The results are shown in Fig. 4(a). For short pulses, we observe that

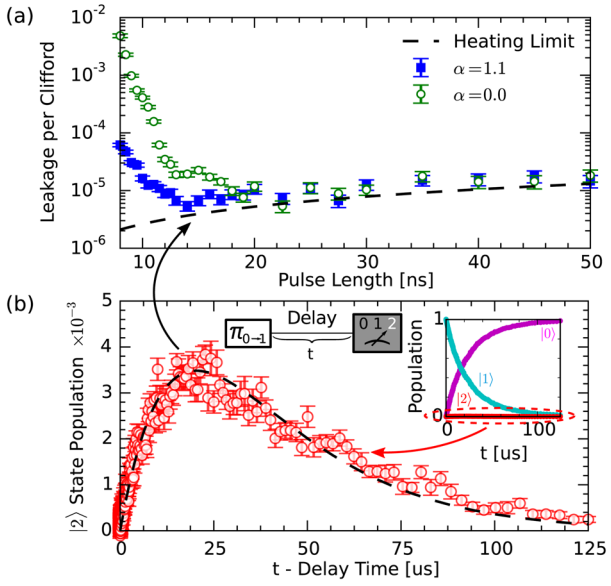

FIG. 4. (a) Leakage rate per Clifford extracted from RB versus pulse length, with $\alpha = 0.0$ and $\alpha = 1.1$. The dashed line is the lower bound on leakage calculated from the heating rate. (b) Heating of the qubit from $|1\rangle$ to $|2\rangle$. We prepare the qubit in $|1\rangle$, wait for time t, then measure the qubit state. Inset: Dynamics of all three states, primarily showing T_1 decay of $|1\rangle$ to $|0\rangle$. Main figure: Zoom-in of the $|2\rangle$ state dynamics, showing an increase in population due to heating before relaxing back to zero. The data have been corrected for readout visibility. The dashed line is a rate equation fit, from which we extract the heating rate plotted in (a).

the leakage rate decreases exponentially with increasing pulse length, and that DRAG correction suppresses leakage by an order of magnitude or more. However, as the pulse length increases past 15 ns, the leakage rate begins to level off and even begins to increase. Furthermore, DRAG no longer seems to suppress leakage for pulses longer than 20 ns. These results suggest that for long pulses leakage is due to incoherent processes such as thermal excitations or noise at the $1 \leftrightarrow 2$ transition, rather than coherent control errors.

To measure the incoherent leakage rate, we prepare the qubit in the $|1\rangle$ state and measure the qubit's dynamics, as shown in Fig. 4(b). We see that the $|2\rangle$ state population initially rises over 20 μs, corresponding to heating from $|1\rangle$ to $|2\rangle$. Then, the $|2\rangle$ population slowly decays to zero as both excited states relax due to T_1 processes. We model the $|2\rangle$ population using a rate equation with three rates: decay from $|2\rangle$ to $|1\rangle$, decay from $|1\rangle$ to $|0\rangle$, and heating from $|1\rangle$ to $|2\rangle$. We ignore nonsequential transitions since they are suppressed in the nearly harmonic transmon potential [36], as well as heating from $|0\rangle$ to $|1\rangle$ since we assume the initial state is $|1\rangle$. We extract the two decay rates from T_1 measurements, which give $T_1^{|1\rangle} = 22$ μs and $T_1^{|2\rangle} = 18$ μs [37]. We then fit the $1 \rightarrow 2$ heating rate to be $1/(2.2\ \text{ms})$ [18].

We convert this heating rate to a leakage rate per Clifford using the prescription in Ref. [30]. The resulting lower bound on leakage is shown by the dashed line in Fig. 4(a). For pulses longer than 15 ns, we find that the leakage rate is within a factor of 2 of this lower bound, confirming that even at these relatively short time scales we are being limited by incoherent processes. We note that the heating rate and T_1 decay rate are consistent with an equilibrium population of 0.8% for the $|1\rangle$ state [18]. In other works, equilibrium populations closer to 0.1% have been achieved [38], suggesting that incoherent leakage can be reduced through improved thermalization.

In conclusion, we have used single qubit randomized benchmarking to study leakage errors in a superconducting qubit. We showed that simple DRAG correction alone cannot minimize leakage and total gate error simultaneously, but by detuning our pulses, we obtain gates with both high fidelity and low leakage. We also measured the dependence of leakage on pulse length, and found that heating of the qubit is a significant source of leakage in our system. Because RB is platform independent, this method is applicable to other systems provided they have high fidelity measurement of their leakage states. This method can also be extended to two-qubit gates, where entangling interactions can be a significant source of leakage [4].

We thank Tobias Chasseur, Felix Motzoi, and Frank Wilhelm for valuable discussions. This work was supported by Google. Z. C. and C. Q. also acknowledge support from the National Science Foundation Graduate Research Fellowship under Grant No. DGE 1144085. Devices were

made at the UC Santa Barbara Nanofabrication Facility, a part of the NSF-funded National Nanotechnology Infrastructure Network, and at the NanoStructures Cleanroom Facility.

*jmartinis@google.com

[1] D. P. DiVincenzo *et al.*, Fortschr. Phys. **48**, 771 (2000).
[2] J. Schliemann, D. Loss, and A. H. MacDonald, Phys. Rev. B **63**, 085311 (2001).
[3] J. Clarke and F. K. Wilhelm, Nature (London) **453**, 1031 (2008).
[4] J. M. Martinis and M. R. Geller, Phys. Rev. A **90**, 022307 (2014).
[5] J. M. Gambetta, F. Motzoi, S. T. Merkel, and F. K. Wilhelm, Phys. Rev. A **83**, 012308 (2011).
[6] E. Lucero, J. Kelly, R. C. Bialczak, M. Lenander, M. Mariantoni, M. Neeley, A. O'Connell, D. Sank, H. Wang, M. Weides *et al.*, Phys. Rev. A **82**, 042339 (2010).
[7] J. M. Chow, L. DiCarlo, J. M. Gambetta, F. Motzoi, L. Frunzio, S. M. Girvin, and R. J. Schoelkopf, Phys. Rev. A **82**, 040305 (2010).
[8] F. Motzoi, J. M. Gambetta, P. Rebentrost, and F. K. Wilhelm, Phys. Rev. Lett. **103**, 110501 (2009).
[9] S. Sheldon, L. S. Bishop, E. Magesan, S. Filipp, J. M. Chow, and J. M. Gambetta, arXiv:1504.06597.
[10] R. Barends, J. Kelly, A. Megrant, A. Veitia, D. Sank, E. Jeffrey, T. White, J. Mutus, A. Fowler, B. Campbell *et al.*, Nature (London) **508**, 500 (2014).
[11] A. G. Fowler, Phys. Rev. A **88**, 042308 (2013).
[12] J. Ghosh, A. G. Fowler, J. M. Martinis, and M. R. Geller, Phys. Rev. A **88**, 062329 (2013).
[13] J. Kelly, R. Barends, A. Fowler, A. Megrant, E. Jeffrey, T. White, D. Sank, J. Mutus, B. Campbell, Y. Chen *et al.*, Nature (London) **519**, 66 (2015).
[14] E. Knill, D. Leibfried, R. Reichle, J. Britton, R. B. Blakestad, J. D. Jost, C. Langer, R. Ozeri, S. Seidelin, and D. J. Wineland, Phys. Rev. A **77**, 012307 (2008).
[15] E. Magesan, J. M. Gambetta, and J. Emerson, Phys. Rev. Lett. **106**, 180504 (2011).
[16] T. Chasseur and F. Wilhelm, Phys. Rev. A **92**, 042333 (2015).
[17] J. J. Wallman, M. Barnhill, and J. Emerson, Phys. Rev. Lett. **115**, 060501 (2015).
[18] See Supplemental Material at http://link.aps.org/supplemental/10.1103/PhysRevLett.116.020501 for a theoretical discussion of Eq. (2), experimental details, and complementary data, with references to Refs. [19–21].
[19] J. M. Epstein, A. W. Cross, E. Magesan, and J. M. Gambetta, Phys. Rev. A **89**, 062321 (2014).
[20] E. Lucero, M. Hofheinz, M. Ansmann, R. C. Bialczak, N. Katz, M. Neeley, A. D. O'Connell, H. Wang, A. N. Cleland, and J. M. Martinis, Phys. Rev. Lett. **100**, 247001 (2008).
[21] M. Fang, B. Campbell, Z. Chen, B. Chiaro, A. Dunsworth, J. Kelly, A. Megrant, C. Neill, P. O'Malley, C. Quintana *et al.*, in *Proceedings of the APS Meeting, 2015, Abstracts of Contributed Papers* (American Physical Society, New York, 2015), Vol. 1, p. 39002.
[22] J. J. Wallman, M. Barnhill, and J. Emerson, Phys. Rev. Lett. **115**, 060501 (2015).
[23] R. Barends, J. Kelly, A. Megrant, D. Sank, E. Jeffrey, Y. Chen, Y. Yin, B. Chiaro, J. Mutus, C. Neill *et al.*, Phys. Rev. Lett. **111**, 080502 (2013).
[24] J. Koch, T. M. Yu, J. M. Gambetta, A. A. Houck, D. I. Schuster, J. Majer, A. Blais, M. H. Devoret, S. M. Girvin, and R. J. Schoelkopf, Phys. Rev. A **76**, 042319 (2007).
[25] H. Paik, D. Schuster, L. S. Bishop, G. Kirchmair, G. Catelani, A. Sears, B. Johnson, M. Reagor, L. Frunzio, L. Glazman *et al.*, Phys. Rev. Lett. **107**, 240501 (2011).
[26] A. Sears, J. Birenbaum, D. Hover, T. Gudmundsen, A. Kerman, P. Welander, J. L. Yoder, S. Gustavsson, X. Jin, A. Kamal *et al.*, in *Proceedings of the APS Meeting, 2014, Abstracts of Contributed Papers* (American Physical Society, New York, 2014), Vol. 1, p. 28005.
[27] A. Wallraff, D. I. Schuster, A. Blais, L. Frunzio, J. Majer, M. H. Devoret, S. M. Girvin, and R. J. Schoelkopf, Phys. Rev. Lett. **95**, 060501 (2005).
[28] E. Jeffrey, D. Sank, J. Mutus, T. White, J. Kelly, R. Barends, Y. Chen, Z. Chen, B. Chiaro, A. Dunsworth *et al.*, Phys. Rev. Lett. **112**, 190504 (2014).
[29] J. Mutus, T. White, R. Barends, Y. Chen, Z. Chen, B. Chiaro, A. Dunsworth, E. Jeffrey, J. Kelly, A. Megrant *et al.*, Appl. Phys. Lett. **104**, 263513 (2014).
[30] P. O'Malley, J. Kelly, R. Barends, B. Campbell, Y. Chen, Z. Chen, B. Chiaro, A. Dunsworth, A. Fowler, I.-C. Hoi *et al.*, Phys. Rev. Applied **3**, 044009 (2015).
[31] F. Motzoi and F. K. Wilhelm, Phys. Rev. A **88**, 062318 (2013).
[32] A. De, arXiv:1509.07905.
[33] A unitary rotation in a two-level system is parametrized by three values, so by setting amplitude, detuning, and phase we can, in principle, generate any rotation and reduce phase errors to zero [4], with the only error being leakage.
[34] S. Gustavsson, O. Zwier, J. Bylander, F. Yan, F. Yoshihara, Y. Nakamura, T. P. Orlando, and W. D. Oliver, Phys. Rev. Lett. **110**, 040502 (2013).
[35] J. Kelly, R. Barends, B. Campbell, Y. Chen, Z. Chen, B. Chiaro, A. Dunsworth, A. Fowler, I.-C. Hoi, E. Jeffrey *et al.*, Phys. Rev. Lett. **112**, 240504 (2014).
[36] M. J. Peterer, S. J. Bader, X. Jin, F. Yan, A. Kamal, T. J. Gudmundsen, P. J. Leek, T. P. Orlando, W. D. Oliver, and S. Gustavsson, Phys. Rev. Lett. **114**, 010501 (2015).
[37] $T_1^{\vert 1\rangle}$ is not $2T_1^{\vert 2\rangle}$ as might be expected because the transitions are at different frequencies, and T_1 in our system is frequency dependent [23].
[38] X. Y. Jin, A. Kamal, A. P. Sears, T. Gudmundsen, D. Hover, J. Miloshi, R. Slattery, F. Yan, J. Yoder, T. P. Orlando *et al.*, Phys. Rev. Lett. **114**, 240501 (2015).